

## Three-dimensional quantitative structure–activity relationship (3D-QSAR) analyses of choline acetyltransferase inhibitors

Vasudevan Chandrasekaran<sup>a</sup>, Georgia B. McGaughey<sup>b</sup>,  
Chester J. Cavallito<sup>c</sup>, J. Phillip Bowen<sup>a,\*,1</sup>

<sup>a</sup> Center for Biomolecular Structure and Dynamics, Department of Chemistry, University of Georgia, Athens, GA 30602-2556, USA

<sup>b</sup> Merck Research Laboratories, P.O. Box 4, West Point, PA 19486, USA

<sup>c</sup> Adjunct Professor Emeritus, University of North Carolina, Chapel Hill, NC, USA

Received 29 February 2004; received in revised form 29 February 2004; accepted 19 April 2004

Available online 19 May 2004

### Abstract

As a basis for predicting structural features that may lead to the design of more potent and selective inhibitors of choline acetyltransferase (ChAT), the three-dimensional quantitative structure–activity relationship (3D-QSAR) studies were carried out on a series of *trans*-1-methyl-4-(1-naphthylvinyl)pyridinium (MNVP<sup>+</sup>) analogs, which are known ChAT inhibitors. 3D-QSAR studies were carried out using the comparative molecular field analysis (CoMFA) and comparative molecular similarity indices analysis (CoMSIA) methods. Since these inhibitors have extremely shallow potential energy minimum energy wells and low barriers to rotation, two dihedral angles unique to these inhibitors were systematically modified to reflect the energetically preferred conformations as determined by force field calculations. An optimum alignment rule was devised based on the conformations obtained from the molecular mechanics studies, using a common substructure alignment method. The studies involve a set of 21 compounds and experimentally determined molar IC<sub>50</sub> values were used as the dependent variable in the analysis. The 3D-QSAR models have conventional  $r^2$ -values of 0.953 and 0.954 for CoMFA and CoMSIA, respectively; similarly, cross-validated coefficient  $q^2$ -values of 0.755 and 0.834 for CoMFA and CoMSIA, respectively, were obtained. On the basis of these predictive  $r^2$ -values the model was tested using previously determined IC<sub>50</sub> values. CoMSIA 3D-QSAR yielded better results than CoMFA.

© 2004 Elsevier Inc. All rights reserved.

**Keywords:** Choline acetyltransferase inhibitors; 3D-QSAR; CoMFA; CoMSIA; Molecular mechanics

### 1. Introduction

Choline acetyltransferase (ChAT) is an important enzyme in the biosynthesis of acetyl choline. Although the enzyme is well known, there is limited structural information available. Over the years, attempts have been made to gain insights into the ChAT binding cavity through indirect means, primarily by probing the interaction of small molecule inhibitor analogs of *trans*-1-methyl-4-(1-naphthylvinyl)pyridinium (MNVP<sup>+</sup>) and related compounds. Although the direct inhibition of ChAT does not appear to be a viable therapeutic

strategy for various disease states at this time, there has been some interesting speculation that ChAT inhibitors may be useful for nerve gas poisoning. The experimental data based on mouse model studies, seem to suggest that the mechanism may not be directly correlated to ChAT enzyme inhibition. Another intriguing approach of potential therapeutic benefit concerns the use ChAT stimulants to increase the levels of acetyl choline. Regardless of the eventual outcome for potential therapeutic approaches involving ChAT inhibition or stimulation, it is of fundamental importance to have a better understanding of this enzyme.

Significant investments and resources have been made by those involved in computational chemistry and computer-assisted drug design to design compounds that will interact with a particular receptor site when the three-dimensional data available for that receptor site is sparse or lacking

\* Corresponding author. Tel.: +336-334-5714; fax: +336-334-5402.

E-mail address: [bowen@cbsd.chem.uga.edu](mailto:bowen@cbsd.chem.uga.edu) (J.P. Bowen).

<sup>1</sup> Contact address: Department of Chemistry and Biochemistry, University of North Carolina at Greensboro, P.O. Box 26170, Greensboro, NC 27402, USA.

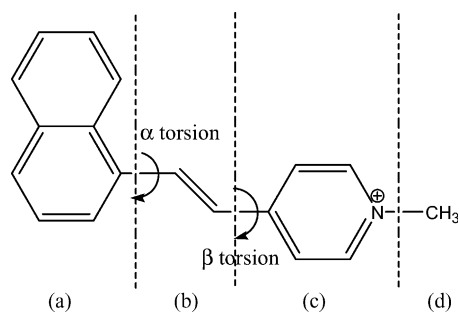


Fig. 1. *trans*-1-Methyl-4-(1-naphthylvinyl)pyridinium.

altogether. Unfortunately, this is the situation that is often found in pharmaceutical research and one medicinal chemists must face. The absence of detailed structural information about the receptor binding site, however, does not preclude the possibility of inferring a pharmacophore model based on only the ligand structure. Three-dimensional quantitative structure activity relationship (3D-QSAR) methods facilitate the correlation of the three-dimensional structures of potential drug molecules with their biological activity and in turn help to predict the activity of new molecules prior to synthesis [1,2]. These methods are based entirely on experimental structure–activity relationships for receptor ligands or enzyme inhibitors, and their application in the last 30 years led to several drugs currently on the market [3–5].

Inhibitors of choline acetyltransferase (ChAT) have been known since the late 1960s. Analogs of *trans*-1-methyl-4-(1-naphthylvinyl)pyridinium (MNVP<sup>+</sup>) (Fig. 1) [6–12] are the simplest and most potent prototype. There are a few known features of MNVP<sup>+</sup> which appear essential for ChAT inhibition. An essentially coplanar conformation of the *trans* **a–b–c** region is believed to be important, although it does not cost much energy to adopt twisted conformations. The feasibility of the co-planarity hypothesis has been supported in an earlier computational chemistry study [10]. Optimum molecular features governing inhibitory potency include region **a** as a bicyclic aryl group or as a phenyl moiety with  $\pi$ -electron donor enhancing substituents, region **b** as a site of unsaturation typically with a double bond (a triple bond, although not used in this study, is also seen) and region **c** as a pyridinium or quinolinium system. Substituents in region **d** are the least structurally refined at this time. The quaternary “onium” forms of these ChAT inhibitors pose limitations in whole animal studies since such ionized species pass through biological membranes with difficulty.

Although ring systems other than pyridinium and quinolinium have been examined (**c** portion of Fig. 1), the MNVP<sup>+</sup> analogs comprise the largest family of molecular variations of ChAT inhibitors and include members for which activities have been confirmed by various researchers [11]. Despite their pharmacological limitations, these compounds still may be useful as biochemical probes to gain further insight into the three-dimensional structure of the neurologically important ChAT enzyme receptor. To provide the highest possible congruency among the compounds included

in this first 3D-QSAR study of MNVP<sup>+</sup> analogs, all of the compounds examined had been assayed for their inhibitory potency by the same procedure [8,9,12].

In this paper, the application of two three-dimensional quantitative structure–activity relationship (3D-QSAR) methods, Comparative molecular field analysis (CoMFA) [13] and comparative molecular similarity indices analysis (CoMSIA) [14,15] for MNVP<sup>+</sup> analogs, as ChAT inhibitors are described. These ligand-based methods of analysis are used widely since they are not very computationally intensive and afford rapid generation of QSAR's from which biological activity of newly designed compounds can be predicted [3]. In order to make use of CoMFA and CoMSIA, the following four procedures are required: (1) superposition of a set of molecules whose activities have been measured; (2) computation of interaction energy fields with various probes; (3) statistical analyses to correlate the fields with activities; and (4) interpretation of the coefficients of the resulting QSAR equations [16].

Based on the alignment of the molecules and the interaction of the steric and electrostatic variables of each molecule with a defined probe atom residing at lattice points in a region in space surrounding the molecules, energy contributions to the interaction between the compounds and the amino acids in the form of lattice points in the active site are sampled. After this region is generated, the results are compared to the pharmacological data, and a linear combination of these two sets of data is constructed using a partial least squares (PLS) algorithm. Cross-validated and non-cross-validated  $r^2$ -values are determined based on the PLS results in order to validate the predictive properties of the model. The  $r^2$ -values can be optimized by iteratively varying the alignment rules, conformations and other parameters inherent to the technique. This general procedure has been used in the present study to gain insight into the steric, the electrostatic, the hydrophobic, the hydrogen-bonding properties of these molecules, their influence on the activity and to derive predictive 3D-QSAR models for design and prediction of the activities of new analogs for this class of inhibitors.

## 2. Materials and methods

### 2.1. Computational details

The molecular modeling software SYBYL 6.9 [17] installed on a Silicon Graphics workstation with IRIX 6.5 operating system, was used for three-dimensional structure generation and molecular modeling studies. The force field calculations used MM3 (2000) with parameters developed for positively charged nitrogen atom and the charges were calculated using the Gasteiger–Huckel method as implemented in SYBYL. The low energy conformers and relative energies for all ChAT inhibitors were examined through dihedral driver optimization technique. The minimum structures were examined, constraints were relaxed and

frequency calculations were carried out to ensure that a global minimum was achieved.

## 2.2. Conformational searching

In the present study, since the structural information on these inhibitor–protein complexes are not available; the conformation of the molecules was obtained from systematic conformational search procedures. The torsion angles  $\alpha$  and  $\beta$  were systematically driven in  $15^\circ$  increments, using the dihedral driver option available in SYBYL (Fig. 1). The low energy conformers were examined and the frequency calculations ensured that the global minimum had been identified on the potential energy surface. It was determined that a low barrier to rotation of both  $\alpha$  and  $\beta$  torsions existed. The torsion angles which reflect the minimum structure demonstrate that all of the compounds in this study exhibited essentially coplanar conformations. These structural observations are consistent with known experimental data in which the *trans* configuration is favored over *cis* configuration [17]. Thus, the coplanar conformations were used for the final 3D-QSAR examination of the compounds.

## 2.3. Structural alignment

The most important requirement for 3D-QSAR techniques (CoMFA and CoMSIA) is that the 3D structures of the molecules to be analyzed be aligned according to a suitable conformational template, which is assumed to adopt a “bio-active conformation” [18]. The molecules in the database were aligned using the “Database Align” routine available in SYBYL. The compounds were fitted to the template molecule 1, one of the most active molecules. The alignment rule was optimized by varying the common substructure used for alignment. As an initial attempt, the structures in the database were aligned by overlaying the carbons in the vinyl linkage. This was thought to be a reasonable approach since this region held the two aromatic moieties together. Another attempt tried to overlay the structures in the database using the pyridinium or quinolinium ring as the backbone. This approach, however, proved to be unproductive. The most successful alignment rule overlaid the atoms of the phenyl moiety in the region **a** (Fig. 1). Such an alignment placed less significance on the region **c** and correspondingly more significance on the region **a** of the MNVP<sup>+</sup> analogs. The entire database was aligned using the coplanar conformations as defined previously and is shown in Fig. 2.

## 2.4. Biological data

The activity data for all the 21 analogs were obtained from the literature reported by Cavallito et al. [8,12]. All of the compounds examined were assayed for their inhibitory potency by the same procedure, to avoid any incongruity of data. The activity data for each compound is listed in Table 1. For this study, the negative log of molar IC<sub>50</sub>

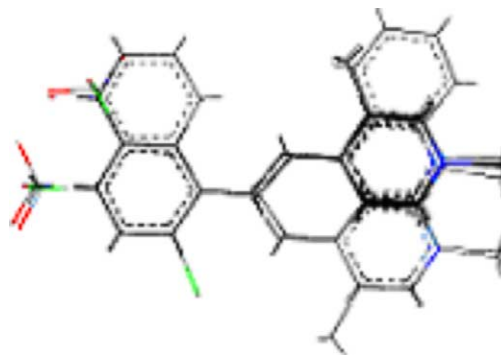


Fig. 2. Alignment of the ChAT inhibitors using common substructure method.

Table 1  
Chat inhibitory activity and Moriguchi log *P* values used in the CoMFA and CoMSIA study

	Compound	–log [molar IC <sub>50</sub> ]	log <i>P</i> <sup>1</sup>
$\text{trans-Ar}-\text{C}(\text{H})=\text{C}(\text{H})-\text{C}_5\text{H}_4\text{N}^+\text{CH}_3\text{I}^-$			
1	1-Naphthyl	6.33	3.75
2	3-BrC <sub>6</sub> H <sub>4</sub>	5.83	3.57
3	3-ClC <sub>6</sub> H <sub>4</sub>	5.64	3.45
4	4-BrC <sub>6</sub> H <sub>4</sub>	5.59	3.57
5	3,4-Cl <sub>2</sub> C <sub>6</sub> H <sub>3</sub>	5.48	3.96
6	4-ClC <sub>6</sub> H <sub>4</sub>	5.16	3.45
7	Phenyl	4.83	2.92
8	4-CH <sub>3</sub> C <sub>6</sub> H <sub>4</sub>	4.70	3.18
9	4-FC <sub>6</sub> H <sub>4</sub>	4.68	3.32
10	2-ClC <sub>6</sub> H <sub>4</sub>	4.56	3.45
11	3-NO <sub>2</sub> C <sub>6</sub> H <sub>4</sub>	3.83	2.76
12	4-NO <sub>2</sub> C <sub>6</sub> H <sub>4</sub>	3.70	2.76
$\text{trans-Ar}-\text{C}(\text{H})=\text{C}(\text{H})-\text{C}_5\text{H}_3(\text{CH}_3)\text{N}^+\text{CH}_3\text{I}^-$			
13	1-Naphthyl	6.40	3.99
14	3-ClC <sub>6</sub> H <sub>4</sub>	5.80	3.70
15	3,4-Cl <sub>2</sub> C <sub>6</sub> H <sub>3</sub>	5.77	4.21
16	Phenyl	5.30	3.18
17	2-ClC <sub>6</sub> H <sub>4</sub>	4.77	3.70
18	3-Indolyl	4.41	2.98
$\text{trans-Ar}-\text{C}(\text{H})=\text{C}(\text{H})-\text{C}_8\text{H}_6\text{N}^+\text{CH}_3\text{I}^-$			
19	Phenyl	5.46	4.15
20	2-Thienyl	3.60	3.35
21	3-Pyridyl	3.22	2.64

( $-\log \text{IC}_{50}$ ) values reported were used, as it would give numerically larger data values for the active compounds than those of the inactive compounds. This is merely a convenience as most of the analysis programs are designed to look for a maximum response. Moriguchi  $\log P$  values were also calculated for each of the compounds in the data set [19,20].

### 2.5. CoMFA and CoMSIA 3D-QSAR models

CoMFA and CoMSIA methods were performed with the QSAR option of SYBYL. For all steps, the default Sybyl settings were used except otherwise noted. In deriving the CoMFA and CoMSIA descriptor fields a 3D cubic lattice with a grid spacing of 2.0 Å in  $x$ ,  $y$  and  $z$  directions was created to encompass the aligned molecules.

The CoMFA steric (Lennard–Jones 6–12 potential) and electrostatic (Coulomb potential) field energies were calculated using  $\text{sp}^3$  carbon probe atom carrying +1 charge, with a distance dependent dielectric at each lattice point. The charges were determined using the Gasteiger–Huckel method. The energy calculation was performed for all grid points such that all energies were constrained to be between  $-30$  and  $+30$  kcal/mol.

CoMSIA descriptors were also derived using the standard implementation in the Sybyl package. Five physicochemical properties (steric, electrostatic, hydrophobic [21], hydrogen bond donor and hydrogen bond acceptor) were evaluated using the probe atom. The probe atom used has a radius of 1 Å, charge of +1, hydrophobicity of +1, and hydrogen bonding and hydrogen donor properties of +1. These fields were selected to cover the major contributions to ligand binding [22]. The default value of 0.3 was used as the attenuation factor ( $\alpha$ ) [15].

A Partial least Squares (PLS) analysis was done to derive the 3D-QSAR models, utilizing the CoMFA standard scaling for the molecular fields. The activity data,  $-\log \text{IC}_{50}$  was used as the dependent variable and the predictive value of the model, represented by  $q^2$ , was evaluated using the leave-one-out (LOO) cross validation method. The optimum number of components was determined based on the standard error of prediction and  $q^2$  values. The equation that gave a low standard error of prediction and high  $q^2$  was chosen. The conventional correlation coefficient  $r^2$  values were also calculated and the incorporation of Moriguchi  $\log P$  values improved the PLS results markedly.

After the 3-D QSAR models were established for our structures, graphical examination of the model depicted which areas around the molecules should contain a greater or lesser amount of electronegative and electropositive groups and whether sterics were an important factor in the inhibition of ChAT. The “Predict Property” command in Sybyl was utilized to determine what the predicted potencies of these compounds were based on the model developed using CoMFA and CoMSIA. The actual and the predicted values of the compounds are listed in Table 3.

### 3. Results and discussion

The 3D-QSAR models which were derived, employing the CoMFA and CoMSIA methods consisting of a set of 21 compounds, (Table 1) must be consistent with the spatial, electronic and other variables that act in concert to provide optimum inhibitory activity. Several of these variables have been identified or proposed for the **a–b–c–d** components of the molecule and for the molecule as a whole [10]. Component **b** which is a *trans*-vinyl linkage and component **d** which primarily serves to quaternize the N atom, do not appear to be structurally specific [23]. This leaves the burden of establishing optimum structural parameters on **a** and **c**.

Apart from CoMFA and CoMSIA descriptor variables, Moriguchi  $\log P$  values for the compounds were included in the development of the models, which complement the field descriptors by correlating with biotransport phenomena rather than specific receptor interactions. This improved the results markedly by giving a higher correlation coefficient. The statistical data obtained from the PLS method for the CoMFA and CoMSIA models is shown in Table 2.

CoMFA models were developed using a common substructure alignment method. The cross-validated  $q^2$ -value from the PLS regression analysis is 0.755, while the non-cross-validated  $r^2$  with five components is 0.953. The actual and predicted values of the activities for the compounds are listed in Table 3.

The CoMFA steric contour plot obtained is shown in Fig. 3. The green (sterically favorable) and yellow (sterically unfavorable) regions in the contour represent 80 and 20% level contributions, respectively. A part of the structure of the most active compounds **1** and **13** protrude into the green (sterically favorable) contour region whereas the other relatively less active compounds do not occupy this region (Fig. 3). The less active compounds either partially touch the

Table 2  
PLS statistical data obtained from the CoMFA and CoMSIA models

PLS statistics	CoMFA	CoMSIA
$q^{2a}$	0.755	0.834
$r^{2b}$	0.953	0.954
ONC <sup>c</sup>	5	5
$F$ -value <sup>d</sup>	53.109	53.737
SEE <sup>e</sup>	0.197	0.196
Field contribution (%) <sup>f</sup>		
log $P$	8.3	22.3
Steric	61.3	9.8
Electrostatic	30.4	18.9
Hydrophobic	–	30.7
H-bond donor	–	6.8
H-bond acceptor	–	11.5

log  $P$ , steric, electrostatic, hydrophobic, H-bond donor–acceptor fields from CoMSIA.

<sup>a</sup> Cross-validated correlation coefficient.

<sup>b</sup> Non-cross-validated correlation coefficient.

<sup>c</sup> Optimal number of components obtained from cross-validated PLS.

<sup>d</sup>  $F$ -test value.

<sup>e</sup> Standard error of estimate.



Table 3  
Results of the predicted activities and residuals of the compounds by the CoMFA and CoMSIA models

Compd	Actual	Predicted (CoMFA)	Residual	Predicted (CoMSIA)	Residual
13	6.40	6.378	0.022	6.503	−0.103
1	6.33	6.343	−0.013	6.318	0.012
2	5.83	5.753	0.077	5.881	−0.051
14	5.80	6.018	−0.218	5.782	0.018
15	5.77	5.681	0.089	5.760	0.010
3	5.64	5.543	0.097	5.582	0.058
4	5.59	5.250	0.340	5.275	0.315
5	5.48	5.503	−0.023	5.563	−0.083
19	5.46	5.440	0.020	5.516	−0.056
16	5.30	5.206	0.094	4.875	0.425
6	5.16	5.099	0.061	5.125	0.035
7	4.83	4.664	0.166	4.646	0.184
17	4.77	4.914	−0.144	4.822	−0.052
8	4.70	4.886	−0.186	4.903	−0.203
9	4.68	4.928	−0.248	4.920	−0.240
10	4.56	4.665	−0.105	4.661	−0.101
18	4.41	4.478	−0.068	4.435	−0.025
11	3.83	4.036	−0.206	3.766	0.064
12	3.70	3.456	0.244	3.907	−0.207

sterically unfavorable regions or do not occupy the sterically favorable region (not shown). The slightly lower activity of **12** as compared to **7** may be due to the fact that *p*-nitro group touches the sterically unfavorable yellow contour region. Thus, the CoMFA steric contours explain the differences in the overall activity of the inhibitors due to differences in spatial arrangement.

The CoMFA electrostatic contour is shown in Fig. 4. The blue (positive charge favored region) and red (negative charge favored region) contours represent 80 and 20% level contribution, respectively. The slightly higher activities of compounds **2** and **3** as compared to **4**, **9** and **10**, although all these compounds have an electronegative group attached to them, is due to the fact that the halogen group in compounds **2** and **3** occupy the red contour region, which is favorable for electronegative groups while the other compounds do not occupy that region. Overall compounds that show relatively

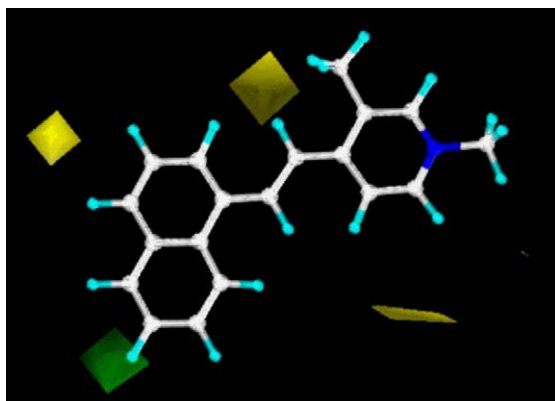


Fig. 3. CoMFA steric S.D.  $\times$  coefficient contour plot; green contours indicate regions where steric bulk is favorable, whereas yellow contours indicate regions where steric bulk is detrimental.

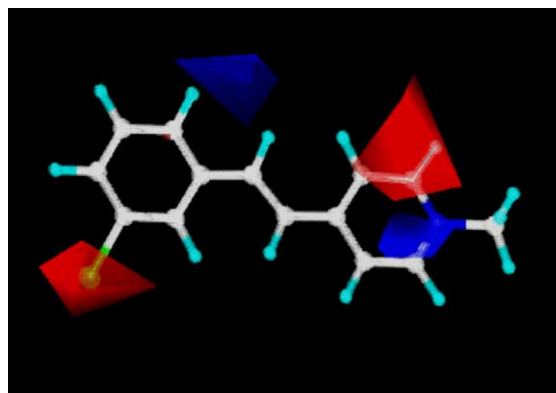


Fig. 4. CoMFA electrostatic S.D.  $\times$  coefficient contour plot; blue contours indicate regions where electropositive groups increase activity, whereas red contours indicate regions where electronegative groups increase activity.

higher activities in the set either have their electronegative group in the red contour or the pyridinium nitrogen near the blue contour.

Component **b** has been well defined where a *trans*-vinyl linkage is optimum. No specific binding contribution can be ascribed to the vinyl bridge other than transmission of electrons between the two rings and facilitation of coplanarity of the inhibitor. It was proposed in an earlier study that the double bond is polarized by a mesomeric interaction with the phenyl ring and the pyridyl ring, causing a partial positive charge on the carbon atom adjacent to the benzene ring and a partial negative charge on the carbon atom adjacent to the pyridyl ring. So, this would enable a nucleophilic residue on the enzyme surface to have a strong interaction with the partial positive charge on the  $\beta$ -carbon to the pyridyl ring [24]. This is evident from the electrostatic contour shown in Fig. 4, where the  $\beta$ -carbon to the pyridyl ring is near the blue contour, consistent with the positive charge.

CoMSIA is similar to CoMFA, but uses a Gaussian function rather than Coulombic and Lennard–Jones potentials to assess the contribution from different fields. Furthermore, in addition to the steric and electrostatic fields of CoMFA, CoMSIA defines explicit hydrophobic and hydrogen bond donor–acceptor fields, which are not available with standard CoMFA. The CoMSIA results gave a cross-validated  $q^2$  value of 0.834, while the non cross-validated  $r^2$  with five components was 0.954. The actual and predicted values of activities for the compounds are listed in Table 3. The CoMSIA steric and electrostatic plots are similar to those obtained from CoMFA. The additional hydrophobic, hydrogen bond donor–acceptor plots are shown in Figs. 5–7, respectively.

The hydrophobic fields (yellow, hydrophobic group favored; white, hydrophobic group disfavored) show that the naphthyl group in the active compounds **13** and **1** fit well into the yellow region which is favorable for hydrophobic groups. While most of the other less active compounds either

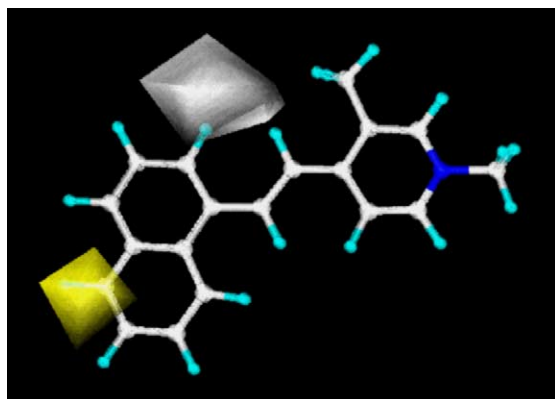


Fig. 5. CoMSIA hydrophobic S.D.  $\times$  coefficient contour plot; yellow contours indicate regions where hydrophobic groups increase activity, white contours indicate regions where hydrophobic groups decrease activity.

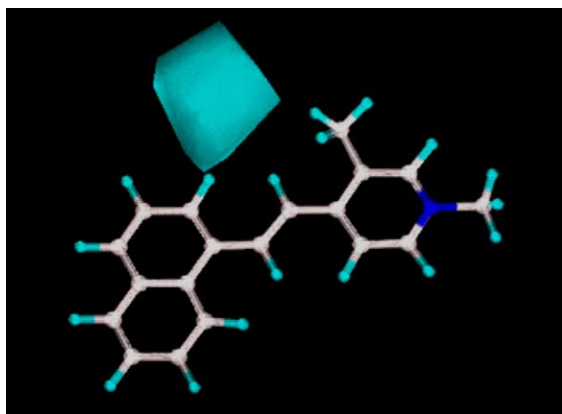


Fig. 6. CoMSIA H-bond donor S.D.  $\times$  coefficient contour plot; cyan contours indicate regions where H-bond donor group increases activity, whereas orange contours indicate regions where H-bond donor group decreases activity.

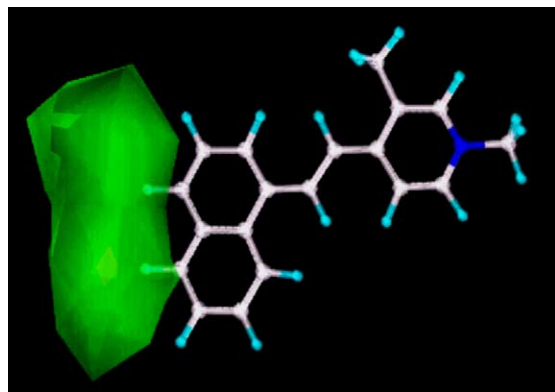


Fig. 7. CoMSIA H-bond acceptor S.D.  $\times$  coefficient contour plots; green contours indicate regions where H-bond acceptor increases activity, whereas red contours indicate regions where H-bond acceptor decreases activity.

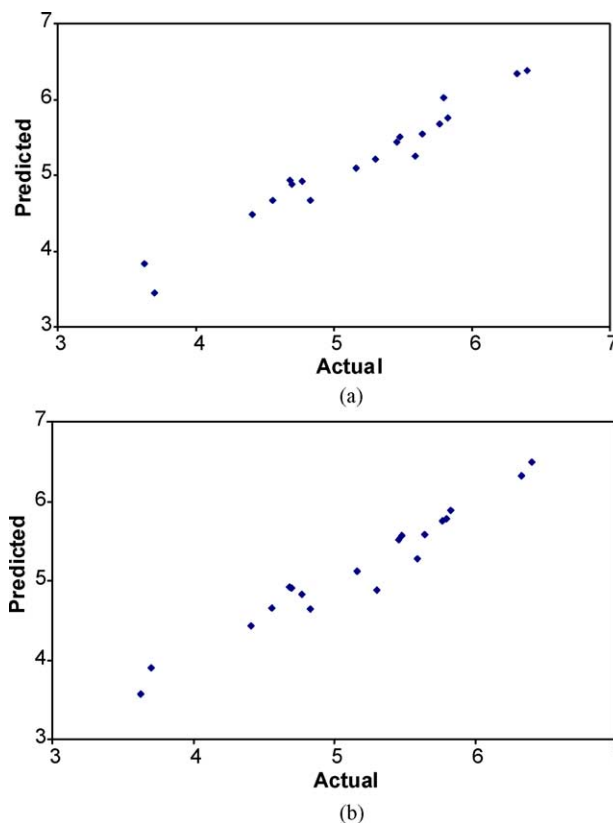


Fig. 8. Comparison of actual vs. predicted  $-\log IC_{50}$  of the molecules for: (a) CoMFA and (b) CoMSIA 3D-QSAR models.

partially touch the yellow contour or occupy unfavorable white region.

With regards to **a**, earlier studies have proposed that substituents enhancing  $\pi$ -donor qualities are favorable for activity [10]. This is clearly seen from the H-bond donor contours (cyan, favored; orange, disfavored) where the aryl group in the region **a** is close to the cyan contour which is favored for activity. The extended naphthyl group at **a** increases the  $\pi$ -donor abilities which could assist in hydrogen bonding to a nearby histidine residue [25]. Thus, overall the CoMSIA fields depict the areas around the molecules where changes either increase or decrease activity. Fig. 8 represents graph of the actual versus predicted  $-\log IC_{50}$  of the molecules for CoMFA and CoMSIA 3D-QSAR models.

The 3D-QSAR models developed were assessed for their predictive abilities using a test set of four compounds, which were not included in the development of the models (Table 4).

The CoMSIA model performed better in predicting the activities than the CoMFA model, possibly because of the inclusion of additional fields to correlate with the activity. The advantage of the ethanol group in these compounds provides adequate aqueous solubility for testing. Variations at this end, especially with extended alkyl groups, may aid in increasing the lipophilicity of these inhibitors. Also, it is

Table 4  
Chat inhibitory activity and Moriguchi log *P* values of the test set molecules

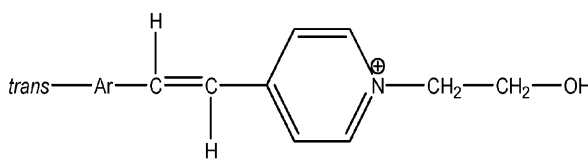
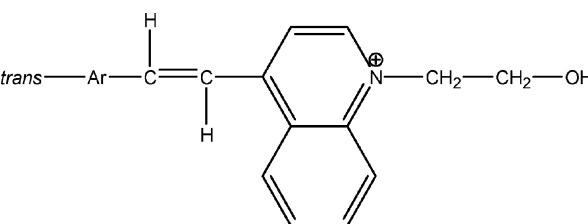
Compound	–log [molar IC <sub>50</sub> ]	log <i>P</i> <sup>1</sup>
		
22 3-BrC <sub>6</sub> H <sub>4</sub>	5.38	3.18
23 3-ClC <sub>6</sub> H <sub>4</sub>	5.62	3.06
		
24 1-Naphthyl	6.28	4.17
25 Phenyl	5.54	3.50

Table 5  
Predicted activities and residuals of the test set by the CoMSIA model

Compd	Actual	Predicted (CoMSIA)	Residual
24	6.28	5.69	0.59
23	5.62	5.28	0.34
25	5.54	5.66	–0.12
22	5.38	5.69	–0.31

conceivable that the alignment of the pyridinium system is not involved in ChAT binding at all. The actual and predicted activities of these compounds are shown in Table 5.

#### 4. Conclusion

We have developed predictive CoMFA and CoMSIA 3D-QSAR models for MNVP<sup>+</sup> analogs as ChAT inhibitors. The CoMSIA model performs better than the CoMFA model in terms of its predictive abilities. These proposed models can be used to predict the activity of newly designed analogs, prior to synthesis. The contour diagrams can be used to identify the structural features of new compounds that would increase or decrease their potency and their activities can be predicted using the QSAR equations. In general, the 3D-QSAR approach gives an insight into the different field contributions around the molecules, and their influence on the overall activity. Further refinement of the structural features might lead to increased potency and aid in increasing the lipophilicity of the molecules. This idea is under investigation in our laboratory.

#### Acknowledgment

This work was carried out at the University of Georgia.

#### References

- [1] Y.C. Martin, P. Willet (Eds.), *Designing Bioactive Molecules: Three-Dimensional Techniques and Applications*, American Chemical Society, Washington, DC, 1998.
- [2] H. Van De Waterbeemd, *Advanced Computer-Assisted Techniques in Drug Discovery*, VCH Publishers, Weinheim, 1995.
- [3] D.B. Boyd, Successes of computer-assisted molecular design, in: K.B. Lipkowitz, D.B. Boyd (Eds.), *Reviews in Computational Chemistry I*, VCH Publishers, New York, 1990, pp. 355–372.
- [4] A. Hillisch, R. Hilgenfeld, The role of protein 3D-structures in the drug discovery process, in: A. Hillisch, R. Hilgenfeld (Eds.), *Modern Methods of Drug Discovery*, Birkhäuser Verlag, Basel, 2003, pp. 157–181.
- [5] J.P. Bowen, Computational chemistry and computer-assisted drug design, in: J.N. Delgado, W.A. Remers (Eds.), *Wilson and Gisvold's Textbook of Organic Medicinal and Pharmaceutical Chemistry*, Lippincott Williams and Wilkins, Philadelphia, 2004, pp. 991–1047.
- [6] J.C. Smith, C.J. Cavallito, F.F. Foldes, Choline acetyltransferase inhibitors. Configurational and electronic features of styrylpyridine analogs, *Biochem. Pharmacol.* 16 (1967) 2438–2441.
- [7] C.J. Cavallito, H.S. Yun, J.C. Smith, F.F. Foldes, Choline acetyltransferase inhibitors. Configurational and electronic features of styrylpyridine analogs, *J. Med. Chem.* 12 (1969) 134–138.
- [8] C.J. Cavallito, H.S. Yun, T. Kaplan, J.C. Smith, F.F. Foldes, Choline acetyltransferase inhibitors. Dimensional and substituent effects among styrylpyridine analogs, *J. Med. Chem.* 13 (1970) 221–224.
- [9] C.J. Cavallito, H.S. Yun, N.L. Edwards, F.F. Foldes, Choline acetyltransferase inhibitors. Styrylpyridine analogs with nitrogen-atom modifications, *J. Med. Chem.* 14 (1971) 130–133.
- [10] M. Kontoyianni, G.B. McGaughey, E.L. Stewart, C.J. Cavallito, J.P. Bowen, Molecular modeling studies of some choline acetyltransferase inhibitors, *J. Med. Chem.* 37 (1994) 3128–3131.
- [11] A.P. Gray, R.D. Platz, T.R. Henderson, T.C.P. Chang, K. Takahashi, K.L. Dretchen, Approaches to protection against nerve agent poisoning: (naphthylvinyl)pyridine derivatives as potential antidotes, *J. Med. Chem.* 31 (1988) 807–814.
- [12] R.C. Allen, G.L. Carlson, C.J. Cavallito, Choline acetyltransferase inhibitors. Physicochemical properties in relation to inhibitory activity of styrylpyridine analogs, *J. Med. Chem.* 13 (1970) 909–912.
- [13] R.D. Cramer III, D.E. Patterson, J.D. Bunce, Comparative molecular field analysis (CoMFA). 1. Effect of shape on binding of steroids to carrier proteins, *J. Am. Chem. Soc.* 110 (1988) 5959–5967.
- [14] G. Klebe, U. Abraham, T. Mietzner, Molecular similarity indices in a comparative analysis (CoMSIA) of drug molecules to correlate and predict their biological activity, *J. Med. Chem.* 37 (1994) 4130–4146.
- [15] M. Bohm, J. Stuzerbercher, G. Klebe, 3D-QSAR analyses using CoMFA and CoMSIA to elucidate selectivity differences of inhibitors binding to trypsin, thrombin and factor Xa, *J. Med. Chem.* 42 (1999) 458–477.
- [16] K.W. Lee, J.M. Briggs, Comparative molecular field analysis (CoMFA) study of epothilones-tubulin depolymerization inhibitors: pharmacophore development using 3D-QSAR methods, *J. Computer-Aided Mol. Design.* 15 (2001) 41–55.
- [17] The program SYBYL 6.9 is available from Tripos Inc., South Hanley Road, St. Louis, MO 63144, USA, 1669.
- [18] B. Gopalakrishnan, A. Khandelwal, S.A. Rajjak, N. Selvakumar, J. Das, S. Trehan, J. Iqbal, M.S. Kumar, Three dimensional quantitative structure–activity relationship (3D-QSAR) studies of tricyclic oxazolidinones as antibacterial agents, *J. Bioorg. Med. Chem.* 11 (2000) 2569–2574.

- [19] U. Moriguchi, S. Hirono, Q. Liu, I. Nakagome, H. Hirano, Comparison of reliability of log *P* values for drugs calculated by several methods, *Chem. Pharm. Bull.* 42 (1994) 976–978.
- [20] U. Moriguchi, S. Hirono, Q. Liu, I. Nakagome, Y. Matsushita, Simple method of calculating octanol/water partition coefficient, *Chem. Pharm. Bull.* 40 (1992) 127–139.
- [21] V.N. Viswanadhan, A.K. Ghose, G.R. Revankar, R.K. Robins, Atomic physicochemical parameters for three dimensional structure directed quantitative structure–activity relationships 4. Additional parameters of hydrophobic and dispersive interactions and their application for an automated superposition of certain naturally occurring nucleoside antibiotics, *J. Chem. Inf. Comput. Sci.* 29 (1989) 163–172.
- [22] G. Klebe, U. Abraham, Comparative molecular similarity index analysis (CoMSIA) to study hydrogen bonding properties and to score combinatorial libraries, *J. Computer-Aided Mol. Design* 13 (1999) 1–10.
- [23] J.F. DeBernardis, P. Gifford, M. Risk, R. Ertel, D.J. Abraham, J.F. Siuda, Evaluation of the side arm of (naphthylvinyl)-pyridinium inhibitors of choline acetyltransferase, *J. Med. Chem.* 31 (1988) 117–121.
- [24] B.V.R. Sastry, N. Jaiswal, V. Janson, P.S. Day, R.J. Naukam, Relationships between chemical structure and inhibition of choline acetyltransferase by 2-( $\alpha$ -naphthyl)ethyltrimethylammonium and related compounds, *J. Pharmacol. Res. Commun.* 20 (9) (1988) 751–771.
- [25] L.A. Carhini, L.B. Hersh, Functional analysis of conserved histidines in choline acetyltransferase by site-directed mutagenesis, *J. Neurochemistry* 61 (1983) 247–253.